Technological and Economic Development of Economy
ISSN: 2029-4913 / eISSN: 2029-4921
2022 Volume 28 Issue 4: 1022–1043
https://doi.org/10.3846/tede.2022.16730

MEASURING THE INTER-STRUCTURAL LOW-CARBON ECONOMIC INEQUALITIES FROM PERSPECTIVES OF INDUSTRIAL HETEROGENEITY AND SCALE ECONOMY: A CASE STUDY OF CHINA'S 29 NON-FERROUS METAL INDUSTRIES

Lu-Xuan SUN[1], Miao WANG[2], Yin-Shuang XIA[3], Chao FENG[4*]

[1]*China-UK Low Carbon College, Shanghai Jiao Tong University, Shanghai, China*
[2]*School of Management, Xiamen University, Xiamen, China*
[3]*School of Economics and Management, Tongji University, Shanghai, China*
[4]*School of Economics and Business Administration, Chongqing University, Chongqing, China*

Received 28 August 2021; accepted 27 February 2022; first published online 20 May 2022

Abstract. With the rapid energy consumption increase in China's non-ferrous metal industry (NMI), there are inequalities in energy-related CO_2 emissions among the sub-sectors. In this paper, a meta-frontier decomposition analysis was proposed for decomposing inter-structural low-carbon economic development inequalities among 29 sub-sectors in China's NMI from 2004 to 2018 into 11 components, including four new factors, i.e., energy- and output- oriented technological gaps and scale economies. In addition, an I(CI) index is constructed to measure the inter-inequalities of low-carbon economic development among NMI and decomposed from the static and dynamic perspectives, respectively. Results show that: (1) I(CI) index was in a downward trend during 2004–2010, while remained stable during 2010–2018; (2) the energy-oriented technological gap (ETG) was the key promoters to increase I(CI); (3) the potential energy intensity (PEI) was the primary inhibiting factor for I(CI); (4) the government can reduce the inter-inequalities by narrowing the technological gap and reducing potential energy intensity in the energy market.

Keywords: low-carbon economy, non-ferrous metal industries, decomposition analysis, inter-structural heterogeneities, scale economy.

JEL Classification: Q01, Q43, Q54, Q56.

Introduction

Global economic development has been accompanied by massive energy-related CO_2 emissions, leading to climate change, sea-level rise, and extreme weather, etc. In 2018, China accounted for 29% of global CO_2 emissions, making it the largest CO_2 emitter. However,

*Corresponding author. E-mail: *littlefc@126.com*

China's carbon intensity in 2018 decreased by 45.8% compared to 2005. Carbon intensity can reveal the evolution and predict the development prospects of low-carbon economic development. Since 2000, the carbon intensity of energy consumption has increased significantly in most regions of the world (Raupach et al., 2007). However, China's low-carbon economic policies have been effective, and several studies have demonstrated a decreasing trend in China's carbon intensity (Fang & Deng, 2011; Li et al., 2019; Wang & Wang, 2020). In addition, many scholars have further investigated the driving factors of carbon intensity change in China from the national level (Fan et al., 2007; Wang et al., 2020; Pang et al., 2021) and the provincial level (Huang, 2018; Wu et al., 2019; Pan et al., 2022). Based on the study of carbon intensity evolution, scholars have predicted the future changes in China's carbon intensity (Guo et al., 2016; Chang & Chang, 2016; Li et al., 2017). For example, Wang et al. (2018) predicted that China's carbon intensity would decrease by 42.39%, 43.74%, and 42.67% from the 2005 level under the unconstrained scenario, the policy-constrained scenario, and the minimal external costs of carbon emissions scenario, respectively.

From the above evolutionary studies, scholars have found carbon intensity inequalities in China. For example, Guan et al. (2014) found that China's carbon intensity increased by 3% overall between 2002 and 2009, while the carbon intensity of the dominant sector showed the least change over the study period compared with other sectors. There were many other studies on the inequalities (Zhou et al., 2020; Wang & Zheng, 2020; Lin et al., 2021). To measure the carbon intensity inequalities in China, some studies have constructed inter-provincial Gini coefficients of carbon intensity (Du et al., 2020; Zhang et al., 2020; Cheng et al., 2021). Wu et al. (2018) found that the Gini coefficients steadily increased from 1995 to 2014. It indicated that the inter-provincial carbon intensity inequalities in China were gradually increasing.

To further study the determinants of carbon intensity inequalities, scholars often use Index Decomposition Analysis (IDA) and Structural Decomposition Analysis (SDA) to decompose the carbon intensity inequalities. The SDA method is mainly based on the input-output model to decompose the carbon intensity impact of input-output coefficients. Xiao et al. (2020) used the SDA method to decompose the carbon intensity inequalities among countries globally from 2010 to 2014 and found that the carbon emission coefficient was the main driving factor for inequalities. However, the application of the SDA method must be based on input-output tables, so the data is relatively difficult to obtain. Therefore, the SDA method is often limited by the data. As for the IDA method, it can decompose carbon intensity into the form of cumulative multiplication and then weight it according to the different factors (Wang et al., 2017a; Xu et al., 2021; Tian et al., 2021). Therefore, it can fully decompose without residual values and is simple to use. Based on the IDA method, scholars have found that energy intensity (Li & Ou, 2013; Chen et al., 2019; Chu et al., 2021), scale economy (Li et al., 2016; Song et al., 2019a), energy structure (Wang et al., 2013; Liu & Gong, 2021), and carbon emission efficiency (Yang et al., 2020) are important influencing factors for the carbon intensity inequalities.

The above approaches failed to take into account the impact of technology and efficiency factors on carbon intensity inequalities, which may play important roles (Zheng et al., 2019; Zhou et al., 2019; Zhang & Ke, 2022). However, it can be solved by the production decom-

position analysis (PDA) method, which is able to measure the technology and efficiency effect (Lin & Du, 2014). Based on an integrated decomposition analysis model combining the IDA method and PDA method, Liu et al. (2020) found that potential energy intensity was the main influencing factor on low-carbon development inequalities. In addition, the influencing factors also included the decline of energy intensity and the advances in production technology (Zang et al., 2021).

The non-ferrous metal industry (NMI) is an important basic material industry in China, while the process of mass production and consumption of non-ferrous metals is accompanied by a large amount of CO_2 emissions. According to the China Carbon Accounting Database, from 2000 to 2018, CO_2 emissions from the NMI increased by 580 million tons per year, with an average annual growth rate of 11%. In 2018, the NMI generated about 650 million tons of carbon emissions, accounting for 6.5% of China's total CO_2 emissions. It can be seen that the overall CO_2 emissions of the NMI were large and show a high growth trend. Therefore, it is crucial to clarify the past successes and shortcomings of the low-carbon economic development in NMI. It can provide scientific evidence for China's NMI to propose specific measures for future low-carbon economic development.

The NMI includes smelting industry (SI), mining industry (MI), and alloy manufacturing and rolling processing (AM&RP), which are subdivided into 29 sub-sectors. Since different types of nonferrous metals have different characteristics and production processes, the determinants for the carbon intensity are also different. Therefore, the inequalities of low-carbon development within the NMI are widespread. If it is not controlled, the sub-sectors with high carbon intensity may fall into a vicious circle, thus generating more CO_2 emissions. It is not conducive to the coordinated low-carbon economic development of China's NMI, thereby hindering the completion of CO_2 emissions reduction targets.

As for China's NMI, it is characterized by high energy consumption, high CO_2 emissions, and high carbon intensity (Wang & Chandler, 2010). Studying the evolution of low-carbon economic development in the NMI can help clarify past successes and shortcomings. Therefore, the pathways to implement new low-carbon policies can be found. In studying the low-carbon economic development of the NMI, many scholars have used scenario analysis (Wang et al., 2016), decoupling analysis (Wang & Feng, 2019; Song et al., 2019b), Logarithmic Mean Divisia Index (LMDI) method (Shi & Zhao, 2016; Wang et al., 2017b), SDA method (Huang et al., 2020), and Malmquist analysis (Chen & Lin, 2020). Among them, the decomposition analysis method can be used to study the determinants of carbon intensity changes. For example, Ren and Hu (2012) found that economy size, energy structure, energy intensity, and utility structure had an impact on CO_2 emissions in the NMI. Wang and Feng (2018) used the LMDI method to decompose energy consumption changes into energy structure effect, energy intensity effect, industry structure effect, labor productivity effect, and economy scale effect. It can be seen that the low-carbon economic development of NMI has been widely concerned and studied.

In the aforementioned studies, scholars have found that there were heterogeneities in the low-carbon economic development in China's NMI. However, there is no study on the evolution and its determinants of CO_2 emissions intensity inter-inequalities of China's NMI. Therefore, the contributions of this study come are twofold: (1) this study uses an extended

PDA model to decompose CO_2 emissions intensity inequalities, by considering heterogeneities and scale economy; (2) this study constructs the inter-inequalities index of low-carbon development within China's NMIs and analyzes its determinants from the static and dynamic perspectives, respectively.

The arrangement of other sections in this paper is as follows: Section 1 introduces the Methodology and data; Section 2 carries out the empirical analysis; and the results and policy recommendations are elaborated in the last Section.

1. Methodology and data

The PDA method will be introduced in Sections 1.1; Section 1.2 describes the construction and decomposition of the low-carbon development inter-inequalities index of NMI; and Section 1.3 presents the details on the data source and processing.

1.1. The production-theoretical decomposition analysis (PDA)

Assuming that the overall carbon intensity of NMI is CI_{μ}, and CI_i represents the carbon intensity of the i_{th} sub-sector. It can be decomposed as follows:

$$CI_i = \frac{C_i}{GDP_i} = \sum_j \frac{C_i}{E_{ij}} \times \frac{E_{ij}}{E_i} \times \frac{E_i}{GDP_i} = \sum_j CF_i \times ES_i \times EI_i, \tag{1}$$

where i and j represent the i_{th} sub-sector and the j_{th} fuel type, respectively; C and GDP are the amount of CO_2 emissions and the gross domestic product; E means energy consumption; CF, ES, and EI represent CO_2 emissions factors, energy structure, and energy intensity.

Combined with the distance function, EI_i can be written as follows:

$$\begin{aligned}
EI_i = \frac{E_i}{GDP_i} = \frac{E_i \big/ D^G{}_{E,i}(l_i,k_i,e_i,y_i,c_i \mid CRS)}{GDP_i \big/ D^G{}_{Y,i}(l_i,k_i,e_i,y_i,c_i \mid CRS)} \times \\
\frac{D^G{}_{E,i}(l_i,k_i,e_i,y_i,c_i \mid CRS)}{D^t{}_{E,i}(l_i,k_i,e_i,y_i,c_i \mid CRS)} \times \frac{D^t{}_{E,i}(l_i,k_i,e_i,y_i,c_i \mid CRS)}{D^t{}_{gE,i}(l_i,k_i,e_i,y_i,c_i \mid CRS)} \times \\
\frac{D^t{}_{gE,i}(l_i,k_i,e_i,y_i,c_i \mid CRS)}{D^t{}_{gE,i}(l_i,k_i,e_i,y_i,c_i \mid VRS)} \times D^t{}_{gE,i}(l_i,k_i,e_i,y_i,c_i \mid VRS) \times \\
\frac{D^t{}_{Y,i}(l_i,k_i,e_i,y_i,c_i \mid CRS)}{D^G{}_{Y,i}(l_i,k_i,e_i,y_i,c_i \mid CRS)} \times \frac{D^t{}_{gY,i}(l_i,k_i,e_i,y_i,c_i \mid CRS)}{D^t{}_{Y,i}(l_i,k_i,e_i,y_i,c_i \mid CRS)} \times \\
\frac{D^t{}_{gY,i}(l_i,k_i,e_i,y_i,c_i \mid VRS)}{D^t{}_{gY,i}(l_i,k_i,e_i,y_i,c_i \mid CRS)} \times \frac{1}{D^t{}_{gY,i}(l_i,k_i,e_i,y_i,c_i \mid VRS)} = \\
PEI \times EST \times TGE \times SEE \times PEE \times PT \times TGY \times SYE \times PYE;
\end{aligned} \tag{2}$$

$$\begin{aligned}
CI_i = \frac{C_i}{GDP_i} = \sum_j CF_{ij} \times ES_{ij} \times PEI_i \times EST_i \times TGE_i \times \\
SEE_i \times PEE_i \times PT_i \times TGY_i \times SYE_i \times PYE_i.
\end{aligned} \tag{3}$$

Among them, *CRS* represents the constant return to scale, and *VRS* represents the variable return to scale; $D^{G}_{E,i}(l_i,k_i,e_i,y_i,c_i\,|\,CRS)$ is energy-oriented distance function based on global meta-frontier data envelopment analysis (DEA); $D^{t}_{E,i}(l_i,k_i,e_i,y_i,c_i\,|\,CRS)$ means energy-oriented distance function based on single phase meta-frontier DEA; $D^{t}{}_{gE,i}(l_i,k_i,e_i,y_i,c_i\,|\,CRS)$ and $D^{t}{}_{gE,i}(l_i,k_i,e_i,y_i,c_i\,|\,VRS)$ represent energy-oriented distance function based on single phase group-frontier DEA in CRS and VRS, respectively; $D^{G}_{Y,i}(l_i,k_i,e_i,y_i,c_i\,|\,CRS)$, $D^{t}_{Y,i}(l_i,k_i,e_i,y_i,c_i\,|\,CRS)$, $D^{t}{}_{gY,i}(l_i,k_i,e_i,y_i,c_i\,|\,CRS)$, and $D^{t}{}_{gY,i}(l_i,k_i,e_i,y_i,c_i\,|\,VRS)$ are output-oriented distance functions on corresponding conditions (please refer to the Appendix A for the specific solution process); *CF*, *ES*, *PEI*, *EST*, *ETG*, *SEE*, *PEE*, *PT*, *TGY*, *SYE*, *PYE* represent carbon emissions factor (CF), energy structure (ES), potential energy intensity (PEI), energy-oriented saving technology (EST), energy-oriented technological gap (ETG), energy-oriented scale economy (SEE), energy-oriented pure technical efficiency (PEE), output-oriented technology (PT), output-oriented technological gap (TGY), output-oriented scale economy (SYE), and output-oriented pure technical efficiency (PYE).

The gap between the i_{th} sub-sector and the whole NMI is CIG_i. Based on the extended kaya identity, the *CIG* change period from 0 to t can be decomposed into:

$$\Delta CIG_i = \Delta CI_{\mu} - \Delta CI_i = \Delta CF_{\mu i} + \Delta ES_{\mu i} + \Delta PEI_{\mu i} + \Delta EST_{\mu i} + \Delta TGE_{\mu i} + \Delta SEE_{\mu i} + \Delta PEE_{\mu i} + \Delta PT_{\mu i} + \Delta TGY_{\mu i} + \Delta SYE_{\mu i} + \Delta PYE_{\mu i}. \tag{4}$$

The 11 determinants can be solved by the following equations:

$$\Delta CF_{\mu i} = \sum_i \sum_j L(CIG^t_{\mu,i,j}, CIG^0_{\mu,i,j}) \ln\left(\frac{CF^t_{\mu,i,j}}{CF^0_{\mu,i,j}}\right); \tag{5}$$

$$\Delta ES_{\mu i} = \sum_i \sum_j L(CIG^t_{\mu,i,j}, CIG^0_{\mu,i,j}) \ln\left(\frac{ES^t_{\mu,i,j}}{ES^0_{\mu,i,j}}\right); \tag{6}$$

$$\Delta PEI_{\mu i} = \sum_i \sum_j L(CIG^t_{\mu,i,j}, CIG^0_{\mu,i,j}) \ln\left(\frac{PEI^t_{\mu,i}}{PEI^0_{\mu,i}}\right); \tag{7}$$

$$\Delta EST_{\mu i} = \sum_i \sum_j L(CIG^t_{\mu,i,j}, CIG^0_{\mu,i,j}) \ln\left(\frac{EST^t_{\mu,i}}{EST^0_{\mu,i}}\right); \tag{8}$$

$$\Delta ETG_{\mu i} = \sum_i \sum_j L(CIG^t_{\mu,i,j}, CIG^0_{\mu,i,j}) \ln\left(\frac{ETG^t_{\mu,i}}{ETG^0_{\mu,i}}\right); \tag{9}$$

$$\Delta SEE_{\mu i} = \sum_i \sum_j L(CIG^t_{\mu,i,j}, CIG^0_{\mu,i,j}) \ln\left(\frac{SEE^t_{\mu,i}}{SEE^0_{\mu,i}}\right); \tag{10}$$

$$\Delta PEE_{\mu i} = \sum_i \sum_j L(CIG^t_{\mu,i,j}, CIG^0_{\mu,i,j}) \ln\left(\frac{PEE^t_{\mu,i}}{PEE^0_{\mu,i}}\right); \tag{11}$$

$$\Delta PT_{\mu i} = \sum_i \sum_j L(CIG^t_{\mu,i,j}, CIG^0_{\mu,i,j}) \ln\left(\frac{PT^t_{\mu,i}}{PT^0_{\mu,i}}\right); \tag{12}$$

$$\Delta TGY_{\mu i} = \sum_i \sum_j L(CIG^t_{\mu,i,j}, CIG^0_{\mu,i,j}) \ln\left(\frac{TGY^t_{\mu,i}}{TGY^0_{\mu,i}}\right); \tag{13}$$

$$\Delta SYE_{\mu i} = \sum_i \sum_j L(CIG^t_{\mu,i,j}, CIG^0_{\mu,i,j}) \ln(\frac{SYE^t_{\mu,i}}{SYE^0_{\mu,i}}); \tag{14}$$

$$\Delta PYE_{\mu i} = \sum_i \sum_j L(CIG^t_{\mu,i,j}, CIG^0_{\mu,i,j}) \ln(\frac{PYE^t_{\mu,i}}{PYE^0_{\mu,i}}). \tag{15}$$

The logarithmic mean weight in Eqs (5)–(15) is calculated as follows:

$$L(CIG^t_{\mu,i,j}, CIG^0_{\mu,i,j}) = \begin{cases} \dfrac{CIG^t_{\mu,i,j} - CIG^0_{\mu,i,j}}{\ln CIG^t_{\mu,i,j} - \ln CIG^0_{\mu,i,j}}, CIG^t_{\mu,i,j} \neq CIG^0_{\mu,i,j} \\ CIG^t_{\mu,i,j} \text{ or } CIG^0_{\mu,i,j}, CIG^t_{\mu,i,j} = CIG^0_{\mu,i,j} \end{cases}. \tag{16}$$

1.2. The construction and decomposition of low-carbon development inequalities index in NMI

To measure the inequalities of low-carbon development within NMI, an $I(CI)$ index was constructed, as follows:

$$I(CI) = \sum_i \phi_i \left| CI_\mu - CI_i \right|, \tag{17}$$

where ϕ_i represents the share of the i_{th} sub-sector in the total output of the whole NMI. $I(CI)$ increases with the inequalities. The static index can be decomposed as follows:

$$I(CI) = \sum_i \phi_i \left| CI_\mu - CI_i \right| = \sum_i \phi_i \left| \begin{matrix} \Delta CF_{\mu i} + \Delta ES_{\mu i} + \Delta PEI_{\mu i} + \Delta EST_{\mu i} + \Delta TGE_{\mu i} + \Delta SEE_{\mu i} + \Delta PEE_{\mu i} \\ + \Delta PT_{\mu i} + \Delta TGY_{\mu i} + \Delta SYE_{\mu i} + \Delta PYE_{\mu i} \end{matrix} \right| =$$
$$I_{CF} + I_{ES} + I_{PEI} + I_{EST} + I_{TGE} + I_{SEE} + I_{PEE} + I_{PT} + I_{TGY} + I_{SYE} + I_{PYE}. \tag{18}$$

The dynamic decomposition of this index is as follows (the change period from 0 to t):

$$I(CI)^t - I(CI)^0 = \left[\sum_i \phi^t_i \left| CI^t_\mu - CI^t_i \right| \right] - \left[\sum_i \phi^0_i \left| CI^0_\mu - CI^0_i \right| \right] =$$
$$\Delta I_{CF} + \Delta I_{ES} + \Delta I_{PEI} + \Delta I_{EST} + \Delta I_{TGE} + \Delta I_{SEE} + \Delta I_{PEE} + \Delta I_{PT} + \Delta I_{TGY} + \Delta I_{SYE} + \Delta I_{PYE}. \tag{19}$$

1.3. Data source and processing

(1) Labor force

The annual average number of employees in each sub-sector of NMI is selected as the measurement index. Among them, the data of employees from 2004 to 2011 come from the *Nonferrous Metal Industry Statistical Data Collection*; the data of employees from 2013 to 2016 come from *China Industrial Statistical Yearbook 2013–2017*; the data in 2012 are the average of 2011 and 2013; and the data of employees in 2017 come from the *China Economic Census Yearbook 2018*. Data for 2018 are from *China Nonferrous Metals Industry Yearbook 2019*.

(2) Main business income

The original data of main business income during 2004–2011 come from *Nonferrous Metals Industry Statistical Data Compilation*, and the data during 2012–2017 come from *China*

Industry Statistical Yearbook 2013–2017. Data for 2018 come from *China Nonferrous Metals Industry Yearbook 2019*. Then, this study uses the PPI of smelting industry (SI), mining industry (MI), and alloy manufacturing and rolling processing (AM&RP) to convert the original data into 2004 constant price.

(3) Completed investment

The data from 2004 to 2015 come from the *Statistical Data Collection of Nonferrous Metals Industry*, and the data during 2016–2018 come from the *Statistical Yearbook of China Nonferrous Metals Industry*.

(4) Capital stock

According to Wang and Lin (2017), the perpetual inventory method is used to measure the capital stock data of NMI. The calculation formula is as follows:

$$K_t = K_{t-1}(1-\delta_t) + I_t / P_t. \tag{20}$$

Capital stock in the base period: the average balance of net fixed assets in 2004 is adopted, and the data are from the *Statistical Data Collection of Nonferrous Metals Industry in 2004*. Annual fixed asset price index: the data come from the *National Bureau of Statistics*. Depreciation rate: 9.6% is adopted in all cases. Annual fixed asset investment: the data from 2004 to 2015 are from the *Nonferrous Metals Industry Statistical Data Compilation*, and the data from 2016 to 2018 come from the completed investment in the *Statistical Yearbook of China Nonferrous Metals Industry*.

(5) Energy consumption

The data from 2004 to 2009 and 2012 are from the *Statistical Data Collection of Nonferrous Metals Industry*; the data during 2010–2011 and 2013–2018 are from the *Statistical Yearbook of China Nonferrous Metals Industry*. These data are converted into standard coal equivalent.

(6) CO_2 emissions

According to the algorithm provided by Intergovernmental Panel on Climate Change [IPCC] (2006), the data include CO_2 emissions from fossil energy and electricity. To ensure that the different indicators of each sub-sector are consistent in all years, this study combines silver mining and beneficiation with other precious metal mining and beneficiation into "precious metal mining and beneficiation"; this study merges "mining and beneficiation of radioactive metal ore" into "mining and beneficiation of other rare metal ore"; this study combines copper calendering and aluminum calendering into "calendering of commonly used nonferrous metals"; this study deletes "nonferrous metal casting" and "other nonferrous metal calendaring" in individual years; this study deletes the silicon smelting data due to only a few years have "silicon smelting" data.

2. Empirical analysis

2.1. Analysis of carbon intensity

2.1.1. Carbon intensity analysis at the level of three types of NMI

As can be seen in Figure 1, the carbon intensity change of China's non-ferrous metal industry (NMI) as a whole can be divided into two stages. It continued to decline from 2004 to 2010 and remained stable from 2010 to 2018. During 2004–2010, the carbon intensity of the NMI as a whole decreased from 7.5298 to 2.2983, by 69.48%. The average annual decrease of it was 16.65%. It may be related to the implementation of energy-saving and CO_2 emissions reduction policies such as the China's national energy efficiency standards for the NMI. For example, the NMI saved 14 million tons of standard coal in 2010, reducing CO_2 emissions by 38 million tons compared with 2005. It also achieved an energy-saving rate of 14.1%, exceeding the target of 10%. Li et al. (2018) quantified low-carbon policies in the NMI sector, and the study found that the implementation of these policies can reduce carbon intensity and achieve peak CO_2 targets. From 2010 to 2018, the carbon intensity of the NMI as a whole stabilized at about 2, with a fluctuation of less than 15%. However, there was a growing trend during 2016–2018. It shows that China's NMI is following the path of steady progress in low-carbon development, but still has some potential for optimization. This is consistent with the research results from Lin and Chen (2019), the carbon emission performance of China's NMI shows an upward trend.

By comparing the carbon intensity changes of the three industries in Figure 1, from large to little, they were smelting industry (SI), mining industry (MI), and alloy manufacturing and rolling processing (AM&RP). However, the carbon intensity increase of SI was much larger than that of the other two categories. It may be because that NMI's energy consumption was mainly derived from SI, accounting for about 80% of the total energy consumption of the NMI. As can be seen from Figure 1, the carbon intensity changing trends of the three sub-sectors were essentially the same, with a significant decline from 2004 to 2010, and a stable trend from 2010 to 2018. It indicates that China's low-carbon development policies for NMI have been effective to some extent. However, there were still inequalities between sub-sectors.

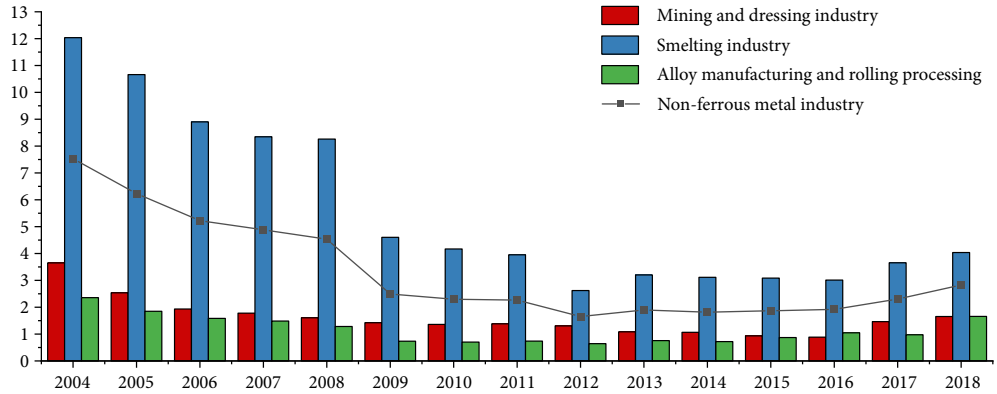

Figure 1. Changes in the carbon intensity of the non-ferrous metal industry from 2004 to 2018

According to Table 1, compared with the NMI as a whole, the change of CO_2 emissions intensity inequalities (CII) of the MI and AM&RP were –2.7019 and –4.0019 (<0), respectively. It indicates that the CII of these two sub-sectors was narrowing. The CII change of SI was 3.3004 (>0), which indicates that SI had an increasing CII and a relatively large space for narrowing it. To further study the determinants, the CII changes of the three sub-sectors from 2004 to 2018 were decomposed into 11 components. As can be seen from Table 1 and Figure 2, PEI had the greatest influence on CII, followed by ETG and SEE. Simultaneously, there was a clear heterogeneity in their effects on different sub-sectors.

From the empirical results of the SI, it is clear that PEI was the main influencing factor for the CII change (Figure 2). It contributes 6.4438 (>0). This indicates that the inequality of

Table 1. The decomposition of carbon intensity inequalities among the three sub-sectors

Decomposition factors	Mining and dressing industry	Smelting industry	Alloy manufacturing and rolling processing
Δtot	–2.7019	3.3004	–4.0019
ΔCF	0.0000	0.0000	0.0000
ΔES	0.8265	–0.1668	0.2066
ΔPEI	–6.9328	6.4488	–7.1398
ΔEST	–3.6097	0.9518	–3.5681
ΔETG	1.2149	–1.8828	5.9936
ΔSEE	4.6028	–3.3792	0.8937
ΔPEE	0.1256	1.3483	–0.6391
ΔPT	–0.2741	0.1499	–0.2062
ΔTGY	1.0713	–0.0478	0.2370
ΔSYE	0.3253	–0.1261	0.2919
ΔPYE	–0.0516	0.0044	–0.0715

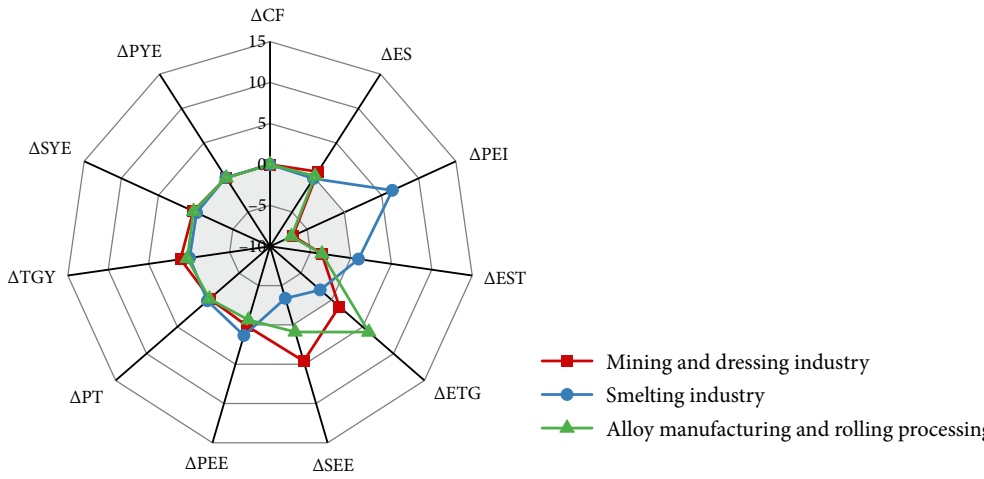

Figure 2. The decomposition of carbon intensity inequalities among the three sub-sectors

potential energy intensity in the SI was very large, which led to the inequality of low-carbon economic development in the SI. However, the impact of PEI on the CII of MI and AM&RP was –6.9328 (<0) and –7.1398 (<0), respectively. Therefore, PEI suppressed the inequality of low-carbon economic development within the two sub-sectors.

However, the impacts of ETG and SEE were the opposite of that of PEI. Compared with the whole NMI, ETG and SEE reduced the CII in SI but increased the CII in MI and AM&RP. It indicates that the CII was due to the very large ETG and SEE inequality between the MI and AM&RP. Further analysis shows that the impacts of PYE on the CII of the three sub-sectors were all smaller than those of PEE. This suggests a potentially more serious misallocation of resources in the energy market. In general, there were significant inequalities in CII changes among different sub-sectors, and the determinants were also heterogeneous.

2.1.2. Decomposition of CII among 29 sub-sectors

According to the above research, there were inequalities of the low-carbon economic development in the three sub-sectors of China's NMI, so 29 sub-sectors were further studied. The 29 sub-sectors are listed in Appendix B. As can be seen from Figure 3, 12 sub-sectors have reduced their carbon intensity more than the NMI as a whole, while 17 sub-sectors have reduced their carbon intensity less than the whole NMI. This indicates that a small number of NMI sub-sectors were more prominent in low carbon performance.

For example, S19, S7, and S18 have reduced their carbon intensity more than the NMI as a whole, especially S19 has been outstanding, which has reduced its carbon intensity by 26.0173 more compared to the NMI as a whole. It indicates that the low carbon development of the magnesium smelting industry performed well in 2004–2018. However, the carbon intensity of S4 has increased by 4.6068 more compared to the industry as a whole.

To further study the determinants of low-carbon development inequalities among 29 sub-sectors. Based on the extended PDA model, the CII change of each sub-sector was decomposed into 11 components, as shown in Table 2. For most of the sub-sectors in the NMI, the factors inhibiting the inequality of low-carbon development were EST, PT, and SYE. Technological change can reduce the carbon intensity of the NMI by reducing energy consumption and optimizing the energy mix (Zhong et al., 2021), so technological change in some sub-sectors can increase the inequality of low-carbon development within the whole industry. However, the factors promoting the inequality of low-carbon development were energy structure, TGY, and PEE. As with the above analysis, the direction and degree of influence of various factors on CII varied across sub-sectors. For example, the impact of PEI on sub-sector S19 was 62.4741, which was much higher than that of others, while the impact of it on sub-sector S26 was –10.0541.

Combined with the above analysis, the high CII of sub-sectors S19, S7, and S18 was mainly due to the large inequality in PEI, contributing 62.4741, 32.0260, and 11.3740, respectively. In analyzing the other decomposition factors for sub-sector S19, it was found that EST had the strongest effect in reducing inequality. The results indicate that the optimization of scale efficiency, production process, production efficiency and energy structure of magnesium smelting reduced inequality. In summary, there was significant heterogeneity in the impact of the decomposition factors on the sub-sectors.

Table 2. Decomposition of CO_2 emissions intensity inequalities among 29 sub-sectors

Industry group	Sub-sectors	Δtot	ΔCF	ΔES	ΔPEI	ΔEST	ΔETG	ΔSEE	ΔPEE	ΔPT	ΔTGY	ΔSYE	ΔPYE
Mining and dressing industry	S1	−1.7930	−0.0002	1.4821	−7.0670	−3.9188	0.2899	5.4253	0.2118	−0.2458	1.0667	0.8200	0.1432
	S2	−3.1498	0.0000	0.6910	−7.7870	−3.0081	0.2244	8.4412	−2.7751	−0.2030	0.9596	0.5673	−0.2601
	S3	4.0605	0.0001	0.4903	7.3728	−5.6928	7.7876	−4.1881	−2.5173	−0.3595	1.7177	−0.2162	−0.3340
	S4	−4.6068	0.0004	0.2079	−9.0846	−2.0092	0.1406	−0.9948	6.9732	−0.1421	0.6187	−0.0236	−0.2932
	S5	6.2165	−0.0001	2.3700	4.1702	−3.8087	0.5822	3.2570	−3.0083	−0.2882	2.1822	1.1156	−0.3555
	S6	1.5024	−0.0006	0.8551	−0.4159	−2.7005	5.5274	−2.1066	−0.5774	−0.2239	1.5834	−0.0450	−0.3935
	S7	22.8568	−0.0001	3.2884	36.0260	−9.0090	1.1107	−7.0389	−5.0053	−1.0850	5.3839	−0.1848	−0.6291
	S8	−0.9582	−0.0001	0.6847	−3.2782	−3.9557	0.3449	−2.1627	6.5035	−0.2564	1.5602	0.0005	−0.3990
	S9	−2.3743	0.0041	0.3615	−5.6299	−2.8146	0.2665	−0.8114	5.5971	−0.2027	1.0332	−0.0472	−0.1308
	S10	−4.0022	−0.0002	0.7582	−9.2236	−3.2374	0.1979	−1.5578	8.0206	−0.2065	0.6414	0.1497	0.4555
	S11	−3.3617	−0.0005	0.1978	−6.8912	−2.6336	0.2149	−0.7157	5.9829	−0.1951	0.8846	−0.8071	0.6013
	S12	2.2172	−0.0005	0.7772	2.2910	−4.5437	8.2056	−3.3372	−2.2780	−0.2899	1.7708	−0.0848	−0.2934
Smelting industry	S13	−3.5191	0.0000	−0.1521	−6.4756	−2.0795	−0.9730	−0.2004	6.3405	−0.1280	−0.0337	−0.0899	0.2726
	S14	0.7202	0.0000	−0.3668	2.6619	−3.9949	−1.9991	−2.8496	7.3082	−0.2928	−0.0715	−0.3192	0.6440
	S15	1.3623	0.0000	−0.3478	3.1707	−3.3862	−2.5894	−0.1536	4.6467	−0.2357	−0.1072	−0.1141	0.4790
	S16	−2.1913	−0.0002	−0.2989	−3.0586	−3.1772	−1.1763	0.8402	4.7680	−0.1958	−0.0353	−0.0774	0.2202
	S17	0.0246	−0.0002	−0.5626	1.3768	−3.0963	−2.1352	3.5907	1.1035	−0.2147	−0.0859	−0.1904	0.2389
	S18	6.2161	0.0000	0.1252	11.3740	3.7591	−0.5975	−5.7688	−2.8218	0.6463	0.0635	−0.1139	−0.4500
	S19	26.0173	−0.0002	−0.8266	62.4741	−16.6528	−4.1924	−8.0118	−5.0473	−0.7340	−0.1178	−0.1913	−0.6827
	S20	1.8253	−0.0002	0.2831	3.0643	−4.5180	−2.1176	2.5458	1.9430	−0.2892	−0.0734	−0.0816	1.0690
	S21	−3.2052	−0.0001	−0.5623	−4.6744	−2.2778	−0.9778	2.2342	3.2985	−0.1579	−0.0323	−0.0394	−0.0160
	S22	−3.8866	−0.0001	−0.3878	−6.4859	−1.6560	−0.9858	6.9827	−0.9214	−0.1297	−0.0378	−0.1488	−0.1160
	S23	−2.9139	0.0000	−0.0522	−5.7346	−2.2312	−1.2979	2.1308	4.1328	−0.1556	−0.0494	−0.0453	0.3886
	S24	0.1692	0.0000	0.3004	−1.2940	−2.8062	−2.5033	1.2402	4.6319	−0.1998	−0.1075	−0.0741	0.9817
	S25	−1.7186	−0.0001	1.5618	−5.9259	−5.5446	−0.3069	0.0210	6.8129	−0.5667	0.0294	−0.4065	2.6069
Alloy manufacturing and rolling processing	S26	−4.5084	0.0000	0.9018	−10.0541	−3.6374	5.6538	−0.4194	2.0131	−0.2064	0.3975	0.2519	0.5909
	S27	−4.0175	0.0000	0.1097	−6.8624	−3.5830	5.8815	1.1219	−0.8343	−0.2061	0.1740	0.3166	−0.1354
	S28	−0.5878	0.0000	−0.3882	−1.2187	−2.1000	10.1388	−5.0167	−1.9726	−0.1985	0.6991	−0.3036	−0.2273
	S29	−3.8526	0.0001	0.3663	−8.1814	−2.5061	5.6395	0.9132	−0.5887	−0.1583	0.3931	−0.0329	0.3025
Values > 0		12	8	19	10	1	16	13	17	1	18	7	14
Values = 0		0	0	0	0	0	0	0	0	0	0	0	0
Values < 0		17	21	10	19	28	13	16	12	28	11	22	15

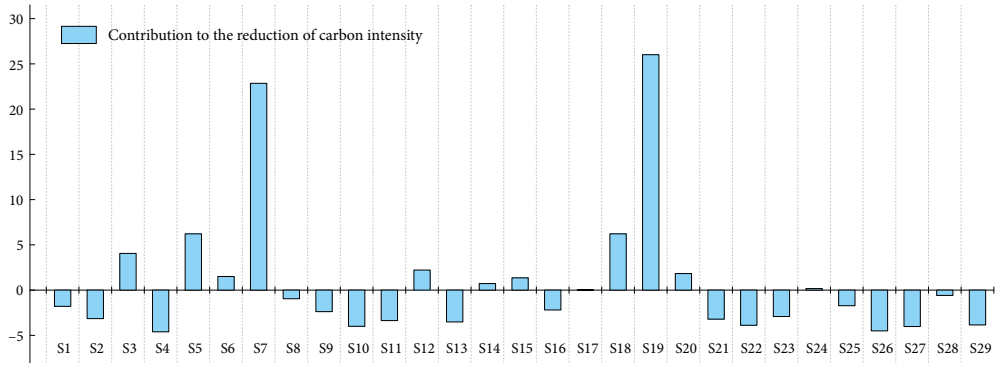

Figure 3. The inequalities of carbon intensity among 29 sub-sectors

2.2. Analysis of inequalities index in NMI

2.2.1. Static analysis

To measure the inequality of low-carbon development within NMI in China, I(CI) was constructed. As shown in Figure 4, the change of I(CI) showed two stages. From 2004 to 2010, the change of I(CI) decreased rapidly from 7.4728 to 2.4989, by 66.56%. It held steady from 2010 to 2018, with fluctuations of no more than 35%. It was similar to the variation of CII described above. This indicates that the inter-inequality of NMI was decreasing and stabilizing at a lower level since 2010. It can be seen from the decomposition results that PEI and PT were the main factors of promoting low-carbon inequality development, while ETG and PEE were the factors to restrain it.

From the perspective of driving factors, PEI was the main factor for the increase of I(CI), accounting for more than 95%. However, after a sharp decline in 2008–2009, its contribution stabilized at a lower level until a slight increase during 2016–2018. To reduce the inequality of low-carbon development in the NMI, there was still a large space to narrow the PEI inequality. PT contributed only second to PEI in promoting I(CI) from 2009 to 2013. Different from PEI, its contribution showed a clear decreasing trend year by year. From the perspective of factors restraining inequality, ETG and PEE contributed to the decline of inequality. However, its contribution gradually decreased. From 2014 to 2018, the main inhibiting factor of I(CI) was EST.

2.2.2. Dynamic analysis

From the dynamic point of view, the ΔI(CI) during the study period in the whole fluctuation was not obvious. From 2008 to 2009, the decline was 47.46%, and the other ranges were no more than 35%. As shown in Figure 5, ΔETG and ΔPEE were the main factors promoting the inter-inequality of low-carbon economic development, ΔPEI was the main factor inhibiting inequality increase. The role of other factors changed over time.

During 2008–2009, it can be seen from Figure 5 that ΔI(CI) was simultaneously affected by the huge impetus of ΔPEI and ΔETG. On the one hand, it may be because of the problem of technological gap. Changes in the energy efficiency technology gap could hinder the low-carbon decoupling process in most sub-sectors except the four major manufacturing and

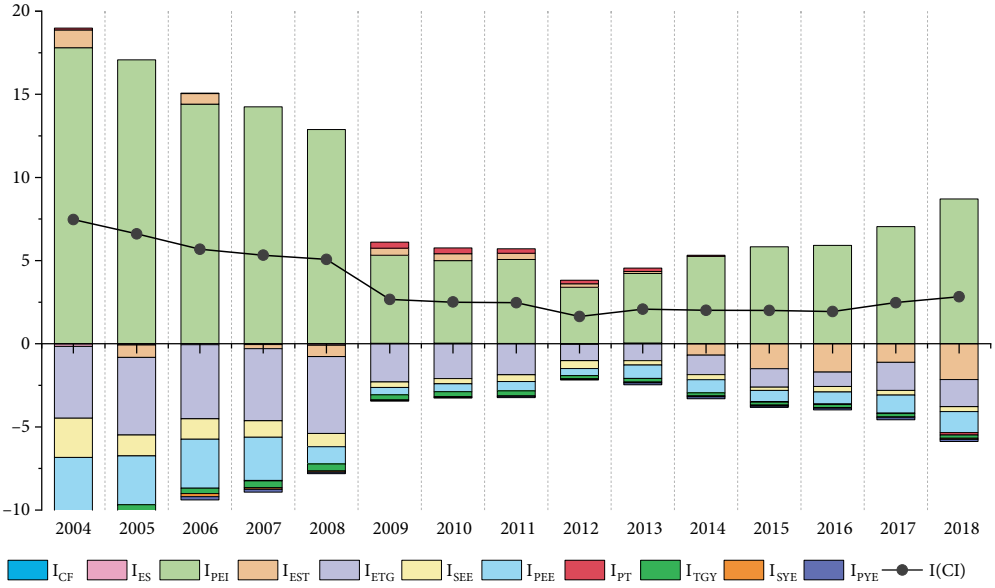

Figure 4. The inequalities index and its decomposition of the non-ferrous metal industry in 2004–2018

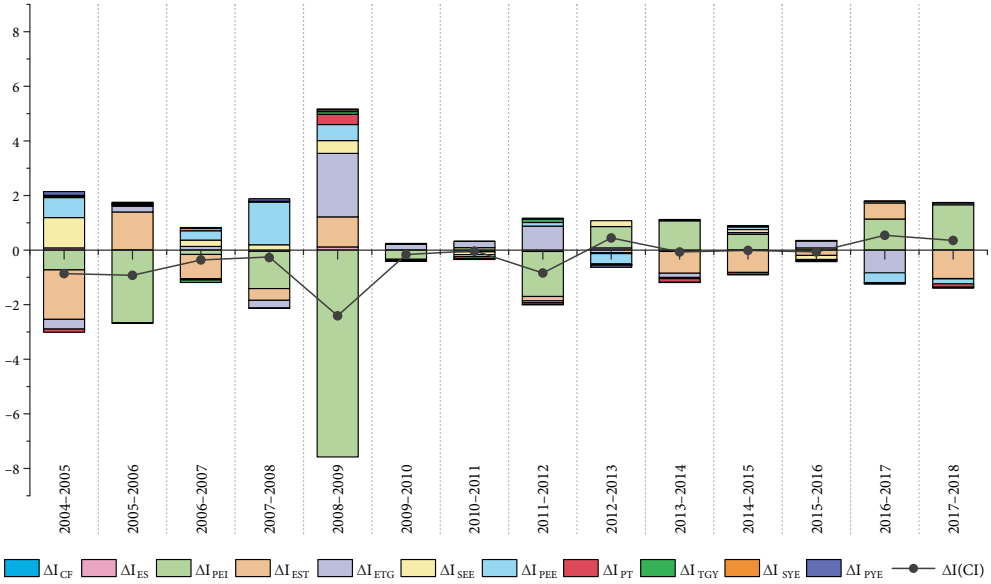

Figure 5. Dynamic change of the inequalities index and its decomposition of the non-ferrous metal industry in 2004–2018

rolling processing industries (Wang & Feng, 2021), which could lead to further inequality. On the other hand, the NMI had the lower potential energy intensity this year. Those two factors simultaneously affected the low-carbon economic development within the NMI during this period, leading to a sharp decline in ΔI(CI). From 2010 to 2018, as mentioned above,

ΔI(CI) remained near 0, indicating that ΔI(CI) was stable and the inequalities of various driving factors changed very little. It was also consistent with the trend of carbon intensity changes in the NMI.

Conclusions and policy recommendations

This paper aims to study the inter-inequalities of low-carbon economic development in the sub-sectors of China's NMI, by using an inequalities index considering heterogeneity and scale economy. Simultaneously, the determinants of the CII of 29 sub-sectors in NMI from 2004 to 2018 were divided into 11 components. Additionally, the I(CI) index was also decomposed from the static and dynamic perspectives, respectively. Results are as follows:

(1) The carbon intensity change in NMI as a whole can be divided into two stages: it continued to decline from 2004 to 2010 and remained stable from 2010 to 2018. During 2004–2010, the carbon intensity decreased from 7.5298 to 2.2983, by 69.48%, with an average annual decrease of 16.65%. During 2010–2018, it stabilized at about 2, with a fluctuation of less than 15%. It shows that China's NMI was following the path of steady progress in low-carbon economic development. However, at the sub-sector level, there were significant inter-inequalities in the NMI. For example, the tin ore selecting (sub-sector S4) had a carbon intensity change of –4.6068, while the carbon intensity of the magnesium smelting (sub-sector S19) increased by 26.0173, much higher than that of the NMI as a whole. Therefore, the Chinese government needs to focus on the inter-inequalities of low-carbon development within the NMI, especially on the production processes with large CO_2 emissions such as magnesium and aluminum sectors, in order to formulate specific low-carbon policies from the perspective of inter-structural inequalities. Among them, the magnesium smelting industry can reduce internal inequality by reducing the potential energy intensity and promoting the advancement of energy-saving technologies.

(2) During the sample period, the EST was the main inhibiting factor for inequalities, followed by PT and SYE. While the adjustment in energy structure and the decline in TGY and PEE were the key promoters. The results suggest that there were significant inequalities in the determinants of CII in China's NMI. Therefore, the Chinese government should take targeted and appropriate measures to improve the situation. For example, the current electricity consumption structure of NMI is still biased towards fossil energy, while the Chinese government should take more measures to narrow the gap between energy structures in order to reduce the inter-inequalities. In addition, the Chinese government can promote market-oriented reforms in the energy sector and narrowed the technology gaps among the sub-sectors of the NMI, therefore the inter-inequalities of low-carbon economic development within NMI can be reduced.

(3) The I(CI) decreased rapidly (–66.56%) from 2004 to 2010, and remained stable (the fluctuation was no more than 35% from 2010 to 2018. It was mainly promoted by ETG and PEE, while PEI was the main inhibiting factor for the I(CI), accounting for more than 85%. However, its contribution had stabilized at a lower level after

decreasing sharply in 2008–2009. Specifically, the PEE was the main promoter during 2004–2009, while an inhibiting factor since 2012. To reduce the I(CI), the Chinese government needs to make further efforts to rationalize the allocation of resources in the energy market and promoting technological progress.

There are two main limitations of this study: (1) this study uses an inequality index to measure the inter-inequalities of low-carbon economic development in China's NMI and decomposes its determinants into 11 components. However, there may be more factors that contribute to the inter-inequalities. Therefore, more factors can be considered in future research; (2) the existence of regional heterogeneity in low-carbon economic development in the NMI has been widely studied, therefore future research could try to consider both inequalities in sub-industries and regional heterogeneity.

Acknowledgements

We gratefully acknowledge financial support from the National Natural Science Foundation of China (No. 72003017), the National Social Science Foundation of China (No. 19ZDA082), and the Fundamental Research Funds for the Central Universities (No. 2021CDJSKCG19).

References

Chang, K., & Chang, H. (2016). Cutting CO_2 intensity targets of interprovincial emissions trading in China. *Applied Energy*, *163*, 211–221. https://doi.org/10.1016/j.apenergy.2015.10.146

Chen, C., Zhao, T., Yuan, R., & Kong, Y. (2019). A spatial-temporal decomposition analysis of China's carbon intensity from the economic perspective. *Journal of Cleaner Production*, *215*, 557–569. https://doi.org/10.1016/j.jclepro.2019.01.073

Chen, X., & Lin, B. (2020). Energy and CO_2 emission performance: A regional comparison of China's non-ferrous metals industry. *Journal of Cleaner Production*, *274*, 123168. https://doi.org/10.1016/j.jclepro.2020.123168

Cheng, S., Fan, W., Zhang, J., Wang, N., Meng, F., & Liu, G. (2021). Multi-sectoral determinants of carbon emission inequality in Chinese clustering cities. *Energy*, *214*, 118944. https://doi.org/10.1016/j.energy.2020.118944

Chu, X., Du, G., Geng, H., & Liu, X. (2021). Can energy quota trading reduce carbon intensity in China? A study using a DEA and decomposition approach. *Sustainable Production and Consumption*, *28*, 1275–1285. https://doi.org/10.1016/j.spc.2021.08.008

Du, Q., Li, J., Li, Y., Huang, N., Zhou, J., & Li, Z. (2020). Carbon inequality in the transportation industry: Empirical evidence from China. *Environmental Science and Pollution Research*, *27*(6), 6300–6311. https://doi.org/10.1007/s11356-019-07291-4

Fan, Y., Liu, L. C., Wu, G., Tsai, H. T., & Wei, Y. M. (2007). Changes in carbon intensity in China: Empirical findings from 1980–2003. *Ecological Economics*, *62*(3–4), 683–691. https://doi.org/10.1016/j.ecolecon.2006.08.016

Fang, Y., & Deng, W. (2011). Affecting elements and regional variables based on the objective of carbon intensity reduction in China. *International Journal of Sustainable Development & World Ecology*, *18*(2), 109–117. https://doi.org/10.1080/13504509.2011.552270

Guan, D., Klasen, S., Hubacek, K., Feng, K., Liu, Z., He, K., Geng, Y., & Zhang, Q. (2014). Determinants of stagnating carbon intensity in China. *Nature Climate Change*, *4*(11), 1017–1023. https://doi.org/10.1038/nclimate2388

Guo, F., Zhao, T., Wang, Y., & Wang, Y. (2016). Estimating the abatement potential of provincial carbon intensity based on the environmental learning curve model in China. *Natural Hazards*, *84*(1), 685–705. https://doi.org/10.1007/s11069-016-2452-4

Huang, J. (2018). Investigating the driving forces of China's carbon intensity based on a dynamic spatial model. *Environmental Science and Pollution Research*, *25*(22), 21833–21843. https://doi.org/10.1007/s11356-018-2307-5

Huang, J. B., Chen, X., & Song, Y. (2020). What drives embodied metal consumption in China's imports and exports. *Resources Policy*, *69*, 101862. https://doi.org/10.1016/j.resourpol.2020.101862

Intergovernmental Panel on Climate Change. (2006). 2006 *IPCC guidelines for national greenhouse gas inventories* (Vol. II). Institute for Global Environmental Strategies, Japan. www.ipcc-nggip.iges.or.jp/public/2006gl/index.html

Li, A., Hu, M., Wang, M., & Cao, Y. (2016). Energy consumption and CO_2 emissions in Eastern and Central China: A temporal and a cross-regional decomposition analysis. *Technological Forecasting and Social Change*, *103*, 284–297. https://doi.org/10.1016/j.techfore.2015.09.009

Li, M., Mi, Z., Coffman, D. M., & Wei, Y. M. (2018). Assessing the policy impacts on non-ferrous metals industry's CO_2 reduction: Evidence from China. *Journal of Cleaner Production*, *192*, 252–261. https://doi.org/10.1016/j.jclepro.2018.05.015

Li, T., Han, D., Feng, S., & Liang, L. (2019). Can industrial co-agglomeration between producer services and manufacturing reduce carbon intensity in China? *Sustainability*, *11*(15), 4024. https://doi.org/10.3390/su11154024

Li, W., & Ou, Q. X. (2013). Decomposition of China's carbon emissions intensity from 1995 to 2010: An extended Kaya identity. *Mathematical Problems in Engineering*, *2013*, 973074. https://doi.org/10.1155/2013/973074

Li, X., Chalvatzis, K. J., & Pappas, D. (2017). China's electricity emission intensity in 2020 – an analysis at provincial level. *Energy Procedia*, *142*, 2779–2785. https://doi.org/10.1016/j.egypro.2017.12.421

Lin, B., & Du, K. (2014). Decomposing energy intensity change: A combination of index decomposition analysis and production-theoretical decomposition analysis. *Applied Energy*, *129*, 158–165. https://doi.org/10.1016/j.apenergy.2014.04.101

Lin, B., & Chen, X. (2019). Evaluating the CO_2 performance of China's non-ferrous metals Industry: A total factor meta-frontier Malmquist index perspective. *Journal of Cleaner Production*, *209*, 1061–1077. https://doi.org/10.1016/j.jclepro.2018.10.278

Lin, Q., Zhang, L., Qiu, B., Zhao, Y., & Wei, C. (2021). Spatiotemporal analysis of land use patterns on carbon emissions in China. *Land*, *10*(2), 141. https://doi.org/10.3390/land10020141

Liu, H., & Gong, G. (2021). Spatial-temporal analysis of China's carbon intensity: A ST-IDA decomposition based on energy input-output table. *Environmental Science and Pollution Research*, *28*(42), 60060–60079. https://doi.org/10.1007/s11356-021-14877-4

Liu, Y., Wang, M., & Feng, C. (2020). Inequalities of China's regional low-carbon development. *Journal of Environmental Management*, *274*, 111042. https://doi.org/10.1016/j.jenvman.2020.111042

Pan, X., Guo, S., Xu, H., Tian, M., Pan, X., & Chu, J. (2022). China's carbon intensity factor decomposition and carbon emission decoupling analysis. *Energy*, *239*, 122175. https://doi.org/10.1016/j.energy.2021.122175

Pang, J., Li, N., Mu, H., Zhanga, M., & Zhao, H. (2021). Study on the spatial interaction between carbon emission intensity and shadow economy in China. *Science of the Total Environment*, 152616. https://doi.org/10.1016/j.scitotenv.2021.152616

Raupach, M. R., Marland, G., Ciais, P., Le Quéré, C., Canadell, J. G., Klepper, G., & Field, C. B. (2007). Global and regional drivers of accelerating CO_2 emissions. *Proceedings of the National Academy of Sciences*, *104*(24), 10288–10293. https://doi.org/10.1073/pnas.0700609104

Ren, S., & Hu, Z. (2012). Effects of decoupling of carbon dioxide emission by Chinese nonferrous metals industry. *Energy Policy*, *43*, 407–414. https://doi.org/10.1016/j.enpol.2012.01.021

Shi, Y., & Zhao, T. (2016). A decomposition analysis of carbon dioxide emissions in the Chinese nonferrous metal industry. *Mitigation and Adaptation Strategies for Global Change*, *21*(6), 823–838. https://doi.org/10.1007/s11027-014-9624-x

Song, C., Zhao, T., & Wang, J. (2019a). Spatial-temporal analysis of China's regional carbon intensity based on ST-IDA from 2000 to 2015. *Journal of Cleaner Production*, *238*, 117874. https://doi.org/10.1016/j.jclepro.2019.117874

Song, Y., Huang, J., Zhang, Y., & Wang, Z. (2019b). Drivers of metal consumption in China: An input-output structural decomposition analysis. *Resources Policy*, *63*, 101421. https://doi.org/10.1016/j.resourpol.2019.101421

Tian, Q., Zhao, T., & Yuan, R. (2021). An overview of the inequality in China's carbon intensity 1997–2016: A Theil index decomposition analysis. *Clean Technologies and Environmental Policy*, *23*, 1581–1601. https://doi.org/10.1007/s10098-021-02050-x

Wang, F., Sun, X., Reiner, D. M., & Wu, M. (2020). Changing trends of the elasticity of China's carbon emission intensity to industry structure and energy efficiency. *Energy Economics*, *86*, 104679. https://doi.org/10.1016/j.eneco.2020.104679

Wang, F., Wang, C., Su, Y., Jin, L., Wang, Y., & Zhang, X. (2017b). Decomposition analysis of carbon emission factors from energy consumption in Guangdong Province from 1990 to 2014. *Sustainability*, *9*(2), 274. https://doi.org/10.3390/su9020274

Wang, J., Zhao, T., & Zhang, X. (2017a). Changes in carbon intensity of China's energy-intensive industries: A combined decomposition and attribution analysis. *Natural Hazards*, *88*(3), 1655–1675. https://doi.org/10.1007/s11069-017-2938-8

Wang, K., Tian, H., Hua, S., Zhu, C., Gao, J., Xue, Y., Hao, J., Wang, Y., & Zhou, J. (2016). A comprehensive emission inventory of multiple air pollutants from iron and steel industry in China: Temporal trends and spatial variation characteristics. *Science of the Total Environment*, *559*, 7–14. https://doi.org/10.1016/j.scitotenv.2016.03.125

Wang, M., & Feng, C. (2018). Decomposing the change in energy consumption in China's nonferrous metal industry: An empirical analysis based on the LMDI method. *Renewable and Sustainable Energy Reviews*, *82*(3), 2652–2663. https://doi.org/10.1016/j.rser.2017.09.103

Wang, M., & Feng, C. (2019). Decoupling economic growth from carbon dioxide emissions in China's metal industrial sectors: A technological and efficiency perspective. *Science of the Total Environment*, *691*, 1173–1181. https://doi.org/10.1016/j.scitotenv.2019.07.190

Wang, M., & Feng, C. (2021). Towards a decoupling between economic expansion and carbon dioxide emissions in resources sector: A case study of China's 29 non-ferrous metal industries. *Resources Policy*, *74*, 102249. https://doi.org/10.1016/j.resourpol.2021.102249

Wang, Q., & Wang, S. (2020). Why does China's carbon intensity decline and India's carbon intensity rise? a decomposition analysis on the sector. *Journal of Cleaner Production*, *265*, 121569. https://doi.org/10.1016/j.jclepro.2020.121569

Wang, X., & Lin, B. (2017). Factor and fuel substitution in China's iron & steel industry: Evidence and policy implications. *Journal of Cleaner Production*, *141*, 751–759. https://doi.org/10.1016/j.jclepro.2016.09.133

Wang, Y., & Chandler, W. (2010). The Chinese nonferrous metals industry – energy use and CO_2 emissions. *Energy Policy*, *38*(11), 6475–6484. https://doi.org/10.1016/j.enpol.2009.03.054

Wang, Y., & Zheng, Y. (2020). Spatial effects of carbon emission intensity and regional development in China. *Environmental Science and Pollution Research*, 1–13.

Wang, Y., Shang, P., He, L., Zhang, Y., & Liu, D. (2018). Can China achieve the 2020 and 2030 carbon intensity targets through energy structure adjustment? *Energies*, *11*(10), 2721. https://doi.org/10.3390/en11102721

Wang, Z. C., Mu, H. L., & Li, H. N. (2013). Analysis of China's CO_2 emission and carbon trading potential. *Applied Mechanics and Materials*, *281*, 704–709. https://doi.org/10.4028/www.scientific.net/AMM.281.704

Wu, R., Dong, J., Zhou, L., & Zhang, L. (2018). Regional distribution of carbon intensity and its driving factors in China: An empirical study based on provincial data. *Polish Journal of Environmental Studies*, *27*(3), 1331–1341. https://doi.org/10.15244/pjoes/76364

Wu, Y., Shen, L., Zhang, Y., Shuai, C., Yan, H., Lou, Y., & Ye, G. (2019). A new panel for analyzing the impact factors on carbon emission: A regional perspective in China. *Ecological Indicators*, *97*, 260–268. https://doi.org/10.1016/j.ecolind.2018.10.006

Xiao, H., Sun, K., Tu, X., Bi, H., & Wen, M. (2020). Diversified carbon intensity under global value chains: A measurement and decomposition analysis. *Journal of Environmental Management*, *272*, 111076. https://doi.org/10.1016/j.jenvman.2020.111076

Xu, S. C., Zhou, Y. F., Feng, C., & Zhang, J. N. (2021). The factors of regional $PM_{2.5}$ emissions inequality in China. *Process Safety and Environmental Protection*, *150*, 79–92. https://doi.org/10.1016/j.psep.2021.04.005

Yang, F., Chou, J., Dong, W., Sun, M., & Zhao, W. (2020). Adaption to climate change risk in eastern China: Carbon emission characteristics and analysis of reduction path. *Physics and Chemistry of the Earth, Parts A/B/C*, *115*, 102829. https://doi.org/10.1016/j.pce.2019.102829

Zang, H., Wang, M., & Feng, C. (2021). What determines the climate mitigation process of China's regional industrial sector? *Environmental Science and Pollution Research*, *28*(8), 9192–9203. https://doi.org/10.1007/s11356-020-11006-5

Zhang, H., & Ke, H. (2022). Spatial spillover effects of directed technical change on urban carbon intensity, based on 283 cities in China from 2008 to 2019. *International Journal of Environmental Research and Public Health*, *19*(3), 1679. https://doi.org/10.3390/ijerph19031679

Zhang, L., Chen, D., Peng, S., Pang, Q., & Li, F. (2020). Carbon emissions in the transportation sector of Yangtze River Economic Belt: Decoupling drivers and inequality. *Environmental Science and Pollution Research*, *27*(17), 21098–21108. https://doi.org/10.1007/s11356-020-08479-9

Zheng, J., Mi, Z., Coffman, D. M., Shan, Y., Guan, D., & Wang, S. (2019). The slowdown in China's carbon emissions growth in the new phase of economic development. *One Earth*, *1*(2), 240–253. https://doi.org/10.1016/j.oneear.2019.10.007

Zhong, M. R., Xiao, S. L., Zou, H., Zhang, Y. J., & Song, Y. (2021). The effects of technical change on carbon intensity in China's non-ferrous metal industry. *Resources Policy*, *73*, 102226. https://doi.org/10.1016/j.resourpol.2021.102226

Zhou, X., Zhou, D., Wang, Q., & Su, B. (2020). Who shapes China's carbon intensity and how? A demand-side decomposition analysis. *Energy Economics*, *85*, 104600. https://doi.org/10.1016/j.eneco.2019.104600

Zhou, Y., Xu, Y., Liu, C., Fang, Z., & Guo, J. (2019). Spatial effects of technological progress and financial support on China's provincial carbon emissions. *International Journal of Environmental Research and Public Health*, *16*(10), 1743. https://doi.org/10.3390/ijerph16101743

APPENDIX

A. Specific solution process

Energy-oriented distance function based on global meta-frontier DEA $\left(D^{G}_{E,i}(l_i,k_i,e_i,y_i,c_i \mid CRS)\right)$ and the corresponding output-oriented distance function $\left(D^{G}_{Y}(l^t,k^t,e^t,y^t,c^t \mid CRS)\right)$ can be solved by the following linear programming:

$$\begin{cases} \dfrac{1}{D^{G}_{E}(l^t,k^t,e^t,y^t,c^t \mid CRS)} = \min\theta \\ \text{s.t.} \sum\limits_{t=0}^{T}\sum\limits_{n=1}^{N} z_n^t \cdot x_n^t \le l^t; \sum\limits_{t=0}^{T}\sum\limits_{n=1}^{N} z_n^t \cdot e_n^t \le \theta e^t; \sum\limits_{t=0}^{T}\sum\limits_{n=1}^{N} z_n^t \cdot k_n^t \le k^t; \\ \sum\limits_{t=0}^{T}\sum\limits_{n=1}^{N} z_n^t \cdot y_n^t \ge y^t; \sum\limits_{t=0}^{T}\sum\limits_{n=1}^{N} z_n^t \cdot c_n^t = \delta c^t; 0 \le \delta \le 1; \\ z_n^t \ge 0, \text{ for } \forall n = 1,2, \cdots, N \text{ and } t = 1,2, \cdots, T. \end{cases} \tag{A.1}$$

$$\begin{cases} \dfrac{1}{D^{G}_{Y}(l^t,k^t,e^t,y^t,c^t \mid CRS)} = \max\eta \\ \text{s.t.} \sum\limits_{t=0}^{T}\sum\limits_{n=1}^{N} z_n^t \cdot x_n^t \le l^t; \sum\limits_{t=0}^{T}\sum\limits_{n=1}^{N} z_n^t \cdot e_n^t \le e^t; \sum\limits_{t=0}^{T}\sum\limits_{n=1}^{N} z_n^t \cdot k_n^t \le k^t; \\ \sum\limits_{t=0}^{T}\sum\limits_{n=1}^{N} z_n^t \cdot y_n^t \ge \eta y^t; \sum\limits_{t=0}^{T}\sum\limits_{n=1}^{N} z_n^t \cdot c_n^t = \delta c^t; 0 \le \delta \le 1; \\ z_n^t \ge 0, \text{ for } \forall n = 1,2, \cdots, N \text{ and } t = 1,2, \cdots, T. \end{cases} \tag{A.2}$$

Energy-oriented distance function based on single phase meta-frontier DEA $\left(D^{t}_{E}(l^t,k^t,e^t,y^t,c^t \mid CRS)\right)$ and the corresponding output-oriented distance function $\left(D^{t}_{Y}(l^t,k^t,e^t,y^t,c^t \mid CRS)\right)$ can be solved by the following linear programming:

$$\begin{cases} \dfrac{1}{D^{t}_{E}(l^t,k^t,e^t,y^t,c^t \mid CRS)} = \min\theta \\ \text{s.t.} \sum\limits_{n=1}^{N} z_n^t \cdot x_n^t \le l^t; \sum\limits_{n=1}^{N} z_n^t \cdot e_n^t \le \theta e^t; \sum\limits_{n=1}^{N} z_n^t \cdot k_n^t \le k^t; \\ \sum\limits_{n=1}^{N} z_n^t \cdot y_n^t \ge y^t; \sum\limits_{n=1}^{N} z_n^t \cdot c_n^t = \delta c^t; 0 \le \delta \le 1; \\ z_n^t \ge 0, \text{ for } n = 1,2, \cdots, N. \end{cases} \tag{A.3}$$

$$\begin{cases} \dfrac{1}{D^t{}_Y(l^t,k^t,e^t,y^t,c^t\,|CRS)}=\max\eta \\ \text{s.t.}\ \sum\limits_{n=1}^{N} z_n^t\cdot l_n^t\le l^t;\sum\limits_{n=1}^{N} z_n^t\cdot k_n^t\le k^t;\sum\limits_{n=1}^{N} z_n^t\cdot e_n^t\le e^t; \\ \sum\limits_{n=1}^{N} z_n^t\cdot y_n^t\ge \eta y^t;\sum\limits_{n=1}^{N} z_n^t\cdot c_n^t=\delta c^t;0\le\delta\le 1; \\ z_n^t\ge 0,\ \text{for}\ n=1,2,\ \cdots,N. \end{cases} \tag{A.4}$$

Under the assumption of constant returns to scale, energy-oriented distance function based on single phase group-frontier DEA $\left(D^t{}_{gE,i}(l_i,k_i,e_i,y_i,c_i\,|CRS)\right)$ and the corresponding output-oriented distance function $\left(D^t{}_{gY}(l^t,k^t,e^t,y^t,c^t\,|CRS)\right)$ can be solved by the following linear programming:

$$\begin{cases} \dfrac{1}{D^t{}_{gE}(l^t,k^t,e^t,y^t,c^t\,|CRS)}=\min\theta \\ \text{s.t.}\ \sum\limits_{n=1}^{N_g} z_n^t\cdot x_n^t\le l^t;\sum\limits_{n=1}^{N_g} z_n^t\cdot e_n^t\le \theta e^t;\sum\limits_{n=1}^{N_g} z_n^t\cdot k_n^t\le k^t; \\ \sum\limits_{n=1}^{N_g} z_n^t\cdot y_n^t\ge y^t;\sum\limits_{n=1}^{N_g} z_n^t\cdot c_n^t=\delta c^t;0\le\delta\le 1; \\ z_n^t\ge 0,\ \text{for}\ \forall n=1,2,\ \cdots,N_g. \end{cases} \tag{A.5}$$

$$\begin{cases} \dfrac{1}{D^t{}_{gY}(l^t,k^t,e^t,y^t,c^t\,|CRS)}=\max\eta \\ \text{s.t.}\ \sum\limits_{n=1}^{N_g} z_n^t\cdot x_n^t\le l^t;\sum\limits_{n=1}^{N_g} z_n^t\cdot e_n^t\le e^t;\sum\limits_{n=1}^{N_g} z_n^t\cdot k_n^t\le k^t; \\ \sum\limits_{n=1}^{N_g} z_n^t\cdot y_n^t\ge \eta y^t;\sum\limits_{n=1}^{N_g} z_n^t\cdot c_n^t=\delta c^t;0\le\delta\le 1; \\ z_n^t\ge 0,\ \text{for}\ \forall n=1,2,\ \cdots,N_g. \end{cases} \tag{A.6}$$

Under the assumption of variable returns to scale, energy-oriented distance function based on single phase group-frontier DEA $\left(D^t{}_{gE}(l^t,k^t,e^t,y^t,c^t\,|VRS)\right)$ and the corresponding output-oriented distance function $\left(D^t{}_{gY}(l^t,k^t,e^t,y^t,c^t\,|VRS)\right)$ can be solved by the following linear programming:

$$\begin{cases} \dfrac{1}{D^t{}_{gE}(l^t,k^t,e^t,y^t,c^t\,|VRS)}=\min\theta \\ \text{s.t.}\ \sum\limits_{n=1}^{N_g} z_n^t\cdot x_n^t\le l^t;\sum\limits_{n=1}^{N_g} z_n^t\cdot e_n^t\le \theta e^t;\sum\limits_{n=1}^{N_g} z_n^t\cdot k_n^t\le k^t; \\ \lambda\sum\limits_{n=1}^{N_g} z_n^t\cdot y_n^t\ge y^t;\lambda\sum\limits_{n=1}^{N_g} z_n^t\cdot c_n^t=\delta c^t;\sum\limits_{n=1}^{N_g} z_n^t=1; \\ 0\le\delta\le 1;z_n^t\ge 0,\ \text{for}\ \forall n=1,2,\ \cdots,N_g. \end{cases} \tag{A.7}$$

$$\begin{cases} \dfrac{1}{D^t{}_{gY}(l^t,k^t,e^t,y^t,c^t \mid VRS)} = \max \eta \\ \text{s.t.} \sum\limits_{n=1}^{N_g} z_n^t \cdot x_n^t \le l^t; \sum\limits_{n=1}^{N_g} z_n^t \cdot e_n^t \le e^t; \sum\limits_{n=1}^{N_g} z_n^t \cdot k_n^t \le k^t; \\ \lambda \sum\limits_{n=1}^{N_g} z_n^t \cdot y_n^t \ge \eta y^t; \lambda \sum\limits_{n=1}^{N_g} z_n^t \cdot c_n^t = \delta c^t; \sum\limits_{n=1}^{N_g} z_n^t = 1; \\ 0 \le \delta \le 1; z_n^t \ge 0, \text{ for } \forall n = 1,2, \cdots, N_g. \end{cases} \tag{A.8}$$

By setting $z_n^{'}=\lambda z_n$ and $z_n^{''}=(1-\lambda)z_n$, model (A.7) and model (A.8) can be re-linearized as follows:

$$\begin{cases} \dfrac{1}{D^t{}_{gE}(l^t,k^t,e^t,y^t,c^t \mid VRS)} = \min \theta \\ \text{s.t.} \sum\limits_{n=1}^{N_g} (z'^t_n + z''^t_n) \cdot x_n^t \le l^t; \sum\limits_{n=1}^{N_g} (z'^t_n + z''^t_n) \cdot e_n^t \le \theta e^t; \sum\limits_{n=1}^{N_g} (z'^t_n + z''^t_n) \cdot k_n^t \le k^t; \\ \lambda \sum\limits_{n=1}^{N_g} z'^t_n \cdot y_n^t \ge y^t; \lambda \sum\limits_{n=1}^{N_g} z'^t_n \cdot c_n^t = \delta c^t; \sum\limits_{n=1}^{N_g} (z'^t_n + z''^t_n) = 1; \\ 0 \le \delta \le 1; z'^t_n, z''^t_n \ge 0, \text{ for } \forall n = 1,2, \cdots, N_g. \end{cases} \tag{A.9}$$

$$\begin{cases} \dfrac{1}{D^t{}_{gY}(l^t,k^t,e^t,y^t,c^t \mid VRS)} = \max \eta \\ \text{s.t.} \sum\limits_{n=1}^{N_g} (z'^t_n + z''^t_n) \cdot x_n^t \le l^t; \sum\limits_{n=1}^{N_g} (z'^t_n + z''^t_n) \cdot e_n^t \le e^t; \sum\limits_{n=1}^{N_g} (z'^t_n + z''^t_n) \cdot k_n^t \le k^t; \\ \lambda \sum\limits_{n=1}^{N_g} z'^t_n \cdot y_n^t \ge \eta y^t; \lambda \sum\limits_{n=1}^{N_g} z'^t_n \cdot c_n^t = \delta c^t; \sum\limits_{n=1}^{N_g} (z'^t_n + z''^t_n) = 1; \\ 0 \le \delta \le 1; z'^t_n, z''^t_n \ge 0, \text{ for } \forall n = 1,2, \cdots, N_g. \end{cases} \tag{A.10}$$

Among them, *l*, *k*, *e*, *y*, *c* are respectively labor, capital, energy, economic output, and CO_2 emissions; *z* represents the strength variable of linked input-output data; T means that the sample contains T periods; *N* is the number of decision units contained in the sample; N_g is the number of decision units in the g_{th} group; CRS and VRS represent the assumption of constant return to scale and variable return to scale respectively.

B. Sub-sectors of China's NMI

ID	Sub-sectors
S1	Copper acquisition
S2	Lead zinc ore mining and dressing
S3	Mining and beneficiation of nickel cobalt ore
S4	Tin ore selecting
S5	Antimony acquisition
S6	Aluminum acquisition
S7	Magnesite acquisition
S8	Other commonly used non-ferrous metal mining and beneficiation
S9	Mining and beneficiation of precious metal ore
S10	Tungsten-molybdenum ore mining and dressing
S11	Mining and beneficiation of rare earth metals
S12	Mining and beneficiation of other rare metals
S13	Copper smelting
S14	Lead and zinc smelting
S15	Cobalt nickel smelting
S16	Tin smelting
S17	Antimony smelting
S18	Aluminium smelting
S19	Magnesium smelting
S20	Other commonly used non-ferrous metal smelting
S21	Silver smelting
S22	Smelting of other precious metals
S23	Tungsten molybdenum smelting
S24	Rare earth metal smelting
S25	Smelting of other rare metals
S26	Nonferrous metal alloy manufacturing
S27	Commonly used nonferrous metal calendering processing
S28	Precious metal calendering processing
S29	Calendering processing of rare earth metals